PFC/JA-86-52

Plasma Current Ramp-up and Ohmic-Heating Transformer Recharging Experiments using Lower-Hybrid Waves on the Alcator C Tokamak

Y. Takase, S. Knowlton, and M. Porkolab

Plasma Fusion Center
Massachusetts Institute of Technology
Cambridge, MA 02139

September 1986

Submitted to: Physics of Fluids

This work was supported by the U.S. Department of Energy Contract No. DE-AC02-78ET51013. Reproduction, translation, publication, use and disposal, in whole or in part by or for the United States government is permitted.

Plasma Current Ramp-up and Ohmic-Heating Transformer Recharging Experiments using Lower-Hybrid Waves on the Alcator C Tokamak

Y. Takase, S. Knowlton, and M. Porkolab

Plasma Fusion Center, Massachusetts Institute of Technology

Cambridge, MA 02139

Plasma current ramp-up by lower-hybrid waves in a high density regime ($\overline{n}_e \gtrsim 1 \times 10^{19}\,\mathrm{m}^{-3}$) is investigated on the Alcator C tokamak. A time-averaged ramp-up efficiency $\dot{W}/P_{rf}$ of 20% has been obtained at a density of $\overline{n}_e = 1.6 \times 10^{19}\,\mathrm{m}^{-3}$, where W is the poloidal field energy. The maximum ramp-up efficiency obtainable is lower at higher densities. Ramp-up rates of over 1MA/s can be obtained when rf current ramp-up is applied to an ohmically maintained plasma. Lower-hybrid current drive can also be used to maintain the plasma while recharging the ohmic-heating transformer. The conversion efficiency P_{el}/P_{rf} during recharging is found to be comparable to that during ramp-up.

I. INTRODUCTION

Non-inductive current drive in tokamaks using lower-hybrid waves has been a subject of active research in the past few years. Purely rf driven plasma currents with no inductive power input have been obtained in a number of experiments,[1-3] and the physics of steady state lower-hybrid current drive (LHCD) in the absence of inductive electric field (i.e., $\dot{I}_p = \dot{I}_{OH} = 0$) is relatively well understood.[4] Here, I_p is the plasma current and I_{OH} is the current in the ohmic-heating (OH) primary coil, and the dot indicates the time derivative. By applying larger amounts of rf power than necessary for maintaining a steady state current, the plasma current may be ramped up ($\dot{I}_p > 0$),[5-7] or the OH transformer may be recharged ($\dot{I}_{OH} > 0$).[8] Lower hybrid assisted ramp-up can be used to reduce the volt-second requirements of the OH transformer (or eliminate its use completely, if sufficiently high current ramp-up and current drive efficiencies could be obtained), whereas OH recharging enables cyclic operation[9] (cycling between the high density OH burn phase and the low density recharging phase) of a tokamak reactor. In both of these cases the physics is more complex due to the presence of the inductive electric field opposing the plasma current.[10,11] It is of great interest to investigate the ramp-up and recharging efficiencies in a more reactor relevant, higher density regime compared to the previously reported experiments.[5,8] In particular, the very low density regimes ($\bar{n}_e \lesssim 6 \times 10^{18}\,\mathrm{m}^{-3}$) used in other experiments may not be achievable in reactor-like devices even in the recharging phase of operations. In this paper we present more detailed results from Alcator C on LH current ramp-up than previously presented[6,7] as well as OH recharging experiments at densities $\bar{n}_e \gtrsim 1 \times 10^{19}\,\mathrm{m}^{-3}$. The high frequency (4.6GHz) and high power levels (up to 1.5MW) used in the present experiment enable us to operate at these high densities. Up to three 4×4 waveguide grill

couplers were used to launch the rf power into the plasma. A relative waveguide phasing of $\Delta\phi = 90°$ was used so that a traveling wave $n_\parallel$ spectrum ($n_\parallel \equiv ck_\parallel/\omega$ is the index of refraction parallel to the magnetic field) propagating predominantly in the direction opposite to the plasma current (i.e., in the same direction as the current carrying electrons) is launched.[12,13] Most of the wave power is contained in the region $n_\parallel < 3$ in the positive direction. There is also a significant fraction ($\simeq 30\%$) of power launched in the negative direction with typical $n_\parallel$'s of 4 to 5.

The plan of the paper is as follows: The results of LH current ramp-up experiments are presented and discussed in Sec. II. LH ramp-up results with finite OH input power is discussed in Sec. III. The OH recharging experiment is discussed and compared with the LH ramp-up results in Sec. IV. Finally, the conclusions are given in Sec. V.

II. LOWER HYBRID CURRENT RAMP-UP EXPERIMENTS

The investigation of LH current ramp-up was carried out with $\dot{I}_{OH} = 0$. A typical ramp-up shot is shown in Fig. 1. After plasma initiation, the OH primary coil was open-circuited so that $I_{OH} = \dot{I}_{OH} = 0$ and no inductive input power is supplied by the OH circuit during LH ramp-up. By applying 420kW of rf power into a hydrogen plasma of $\overline{n}_e = 2.3 \times 10^{19}\,\mathrm{m}^{-3}$ and $I_p \simeq 100\,\mathrm{kA}$ at $B = 8.2\,\mathrm{T}$, a ramp-up rate of $\dot{I}_p \simeq 240\,\mathrm{kA/s}$ is obtained. A superthermal electron tail is formed shortly after the application of rf power, and a slow buildup of the electron tail is observed during the current ramp-up as evidenced by the slow increase of the electron cyclotron emission and the plasma hard X-ray Bremsstrahlung emission.[13] The quantity $\beta_p + \ell_i/2$ obtained from the equilibrium analysis shows a slight decrease during the ramp-up, where, $\beta_p = (\beta_{p\parallel} + \beta_{p\perp})/2$ is the poloidal beta (including the contribution from the electron tail), and $\ell_i \equiv \langle B_p(r)^2 \rangle / B_p(a)^2$ is the plasma

internal inductance parameter.

A. Analysis of experimental data

The power flow during LH current ramp-up has been discussed previously by Fisch and Karney,[10] and can be represented schematically by the diagram shown in Fig. 2. A fraction of the input rf power $P_{abs} \equiv \eta_{abs} P_{rf}$ is absorbed by the fast electrons resonant with the wave phase velocity. We have taken into account the direct power loss from the energetic tail electrons which diffuse radially to the edge before slowing down (by either collisions or by the retarding electric field). This power loss, P_{loss}, can be a significant fraction of the input power, especially at low densities,[13,14] and is subtracted from the absorbed power in our analysis. Hence, $P_{in} \equiv \eta_{eff} P_{rf} \equiv P_{abs} - P_{loss}$ represents only that part of the absorbed rf power which is not lost by radial diffusion. Some fraction of P_{in} is dissipated by collisions providing the bulk heating power P_h. The rest of the power P_{el} (defined as $-\int \mathbf{E}\cdot\mathbf{j}_{rf}\, dV$, where $\mathbf{E}$ is the toroidal electric field and $\mathbf{j}_{rf}$ is the rf current density) does work against the negative electric field which develops as a consequence of current ramp-up, contributing to the increase in the poloidal field energy. This inductive electric field provides ohmic heating of the bulk plasma, V^2/R_{Sp} (defined as $\int E^2/\eta_{Sp}\, dV$, where η_{Sp} is the Spitzer resistivity). In addition, the negative electric field may create a runaway tail in the direction opposing the plasma current. The creation of the reverse runaway tail is expected to be unimportant, since in the present experiments $v_{ph}/v_r \lesssim 1$, where $v_{ph} = c/n_{\|}$ is the wave phase velocity and v_r is the runaway velocity.[10] Since the vertical field increases with time in order to maintain equilibrium, there is always a finite external inductive power input P_{ext} contributed from the equilibrium field (EF) circuit.

An equivalent circuit diagram of the plasma is shown in Fig. 3. In this sim-

plified model, profile effects are ignored. We wish to consider the efficiency of converting the rf energy to the poloidal field energy, $W \equiv LI_p^2/2$, where L is the total self inductance of the plasma loop and I_p is the total (rf plus inductive) plasma current. The loop voltage on the plasma is given by $V = V_{ext} - L\dot{I}_p$, where V_{ext} is the inductive voltage contributed from OH primary and EF circuits. Multiplying both sides by I_p and utilizing $I_p = I_{rf} + V/R_{Sp}$, we obtain

$$P_{el} = \dot{W} - P_{ext} + \frac{V^2}{R_{Sp}} \tag{1}$$

where we have rewritten $P_{el} \equiv -VI_{rf}$ and $P_{ext} \equiv V_{ext}I_p$.[10]

There are several ways of defining a figure of merit for current ramp-up, the most obvious of which is $\dot{W}/P_{rf}$. One can argue that the contribution due to P_{ext} (in this case, from the EF circuit) should be subtracted out.[5] However, P_{ext} is required to maintain plasma equilibrium and will always be present, although its magnitude in relation to $\dot{W}$ may be specific to a particular device. Moreover, the ratio $P_{ext}\,/\,\dot{W}$ would be approximately constant if $\dot{\beta}_p$ and $\dot{\ell}_i$ were small, which would be true after the initial transient phase. This ratio is approximately 1/3 in case of Alcator C. The quantity $(\dot{W} - P_{ext})/P_{rf}$ can thus be obtained by multiplying $\dot{W}/P_{rf}$ by 2/3 in our device. In order to compare the present results with the theoretical predictions of Fisch and Karney,[10,15] the efficiency for conversion of wave energy into poloidal field energy, P_{el}/P_{rf}, is also evaluated. In this paper, we shall call P_{el}/P_{rf} the "conversion efficiency"[10] in order to distinguish it from the "ramp-up efficiency", defined as $\dot{W}/P_{rf}$.

The model described above can easily be refined by taking profile effects into account. In the remainder of this sub-section the procedure used in our analysis is outlined. On Alcator C, the loop voltage V_l is measured on the vacuum chamber whose minor radius is $b = 0.192\,\mathrm{m}$, and at the same major radius as the plasma,

$R = 0.64\,\mathrm{m}$. The plasma minor radius is defined by molybdenum limiters of radius $a = 0.165\,\mathrm{m}$. The loop voltage can be expressed as

$$V_l = -M_{l,OH}\dot{I}_{OH} - M_{l,EF}\dot{I}_{EF} - M_{l,p}\dot{I}_p, \tag{2}$$

where the M's represent the mutual inductances between the voltage loop and the OH primary circuit, the EF circuit, and the plasma, respectively. We recognize that $M_{l,p} = L_{ext}$ where $L_{ext} \equiv \mu_0 R[\ln(8R/b) - 2]$ is the plasma self inductance external to the vacuum chamber. Rewriting the first two terms on the right hand side as V_l^{ext}, we have $V_l = V_l^{ext} - L_{ext}\dot{I}_p$. The inward Poynting flux crossing the vacuum chamber can be obtained by multiplying both sides by I_p: $V_l I_p = P_{ext} - \dot{W}_{ext}$ where we have defined $P_{ext} \equiv V_l^{ext} I_p$ and $W_{ext} \equiv L_{ext} I_p^2/2$. This power flux can be equated to $\dot{W}_{int} + \int \mathbf{E}\cdot\mathbf{j}\,dV$, where $W_{int} \equiv L_{int} I_p^2/2$ is the energy stored internal to the vacuum chamber. Dividing the current density into the rf current and the inductive current, $\mathbf{j} = \mathbf{j}_{rf} + \mathbf{E}/\eta_{Sp}$, using $W = W_{int} + W_{ext}$ and the definitions for P_{el} and V^2/R_{Sp} given in the first paragraph of this sub-section, and rewriting the above equality yields Eq. (1).

The total inductance $L = \mu_0 R[\ln(8R/a) + \ell_i/2 - 2]$ and the current profile parameter $\ell_i/2$ were obtained from the equilibrium vertical field through the relationship[16]

$$B_v = -\mu_0 I_p/(4\pi R)[\ln(8R/a) + \beta_p + \ell_i/2 - 3/2]. \tag{3}$$

The value of β_p is not known very accurately, but a reasonable estimate can be made from bulk density and temperature profile measurements, and from the tail energy measurements performed under steady state current drive conditions.[13] Fortunately this uncertainty does not affect the measurement of the inductance greatly since β_p is usually small ($\lesssim 10\%$) compared to $\ell_i/2$, but it can affect the evaluation of $\dot{\ell}_i$

during the tail build-up phase when $\dot{\beta}_p$ is large. The external inductive power P_{ext} was calculated from the currents in the OH primary and the EF circuits.

Under current ramping conditions the loop voltage is not constant across the plasma cross section. In order to estimate the V^2/R_{Sp} term, we infer the current density profile $j(r)$ from $\ell_i/2$ assuming a gaussian profile. The electric field profile can then be calculated as $E(r) = V_l/(2\pi R) - \int_r^b \dot{B}_p\, dr$. The dashed loop voltage trace shown in Fig. 1 is the loop voltage at the plasma center calculated in this way. The V^2/R_{Sp} power is usually negligible compared to the input rf power except during the initial fast ramp-up phase. For the case shown in Fig. 1, V^2/R_{Sp} was less than 10kW during the ramp-up (after the initial transient).

It is important to note that in current ramp-up experiments a constant $\dot{W}/P_{rf}$ cannot be sustained indefinitely with a constant rf power. In general, $\dot{W}$ must asymptote to zero as the plasma current approaches the steady state current that can be maintained by a given amount of rf power. Such a behavior is usually observed experimentally, except for a short transient immediately following the rf turn on. In our analysis, we shall exclude the first 50ms and perform a time average over the following 50ms in order to avoid complications caused by transient effects, which typically lasts for 20–30ms. The transient effects will be discussed later in Sec. II–C.

B. Experimental results

In Fig. 4, $\dot{W}$ and P_{ext} are shown as functions of time for one of the best ramp-up shots obtained on Alcator C. A ramp-up rate in excess of 300kA/s have been obtained at a density of $\overline{n}_e = 1.6 \times 10^{19}\,\mathrm{m}^{-3}$ with 260kW of rf power. The time averaged (after the initial 50ms) powers were $\dot{W} \simeq 60\,\mathrm{kW}$, $P_{ext} \simeq 25\,\mathrm{kW}$, $V^2/R_{Sp} \simeq 8\,\mathrm{kW}$, and the time averaged ramp-up efficiency $\dot{W}/P_{rf}$ was slightly

over 20% ($\dot{W}/P_{rf}$ would be 30% if the first 50ms were included in the time average, as was done in Refs. 5 and 15). This represents one of the best ramp-up efficiencies obtained on Alcator C. The decrease of the ramp-up efficiency with time, mentioned earlier, is evident. Such a behavior is less noticeable when the ramp-up rate is smaller. The apparent sharp decrease of $\dot{W}$ near the end of the rf pulse ($t \gtrsim 290\,\mathrm{ms}$) is caused by filtering (50Hz gaussian filter), and is not real.

In Fig. 5 we show an example of the power dependence of the current ramp-up efficiency $\dot{W}/P_{rf}$. A zero value of $\dot{W}/P_{rf}$ corresponds to a steady state current whereas $\dot{W}/P_{rf} < 0$ corresponds to a decaying current. We see that $\dot{W}/P_{rf}$ does not keep increasing with power, but saturates and even deteriorates slightly at higher powers. The maximum value of $\dot{W}/P_{rf}$ is achieved at a power level typically two to three times the power needed to maintain a steady state current. The maximum ramp-up efficiency $\dot{W}/P_{rf}$ obtained at each density (at power levels two to three times the steady state value) is shown as a function of density in Fig. 6. It can be seen that the highest value of ramp-up efficiency of $\dot{W}/P_{rf} \simeq 20\%$ is obtained at low densities ($\overline{n}_e \simeq 1 \times 10^{19}\,\mathrm{m}^{-3}$), and the maximum achievable ramp-up efficiency decreases at higher densities. The deterioration of the ramp-up efficiency at higher densities is not due to power limitations, but the exact cause is presently not well understood.

To compare these results with the theory of Fisch and Karney,[10,15] we examine the dependence of P_{el}/P_{in} on v_{ph}/v_r, where $v_r = \pm\sqrt{ne^3 \log\Lambda/(4\pi\epsilon_0^2\,|E|\,m_e)}$ with $v_r > 0$ for $E < 0$ (ramp-up) and $v_r < 0$ for $E > 0$ (rampdown). The value of v_r at the plasma center is used since current carrying fast electrons are concentrated near the plasma center, as evidenced by plasma hard X-ray profile measurements.[17]

The time averaged conversion efficiencies, $P_{el}/P_{rf} = \eta_{eff} P_{el}/P_{in}$, of nearly 200 shots are displayed in Fig. 7(a), compared with the theoretical curve given by

Fisch and Karney[10]. We have chosen the values for the two adjustable parameters to be $\eta_{eff} \equiv P_{in}/P_{rf} = 0.6$ and $\langle n_{\|} \rangle = 3$ in order to fit the theoretical curve to the experimental data points. The value of $\langle n_{\|} \rangle$ represents an effective value of $n_{\|}$ to be used if the spectrum of waves absorbed by the plasma were to be replaced by a single wave. The value of Z_{eff} was measured by visible Bremsstrahlung to be approximately 3 in these ramp-up plasmas. The time average was performed for 50ms after the first 50ms in order to eliminate transient effects, as discussed earlier. Such an effective absorption efficiency is consistent with a nearly complete absorption of the waves by the high energy electrons ($\eta_{abs} > 0.9$) and a direct power loss from the tail of one-third to one-half of the absorbed power, estimated under similar conditions.[13,14] (Note that η_{eff} represents only that part of the absorbed power which ends up as P_{el} or P_h.) However, we note that an equally good fit can be obtained with $\eta_{eff} = 1.0$ and $\langle n_{\|} \rangle = 4$, as shown in Fig. 7(b). The fit becomes significantly worse if η_{eff} is chosen to be less than 0.5. The value of $\langle n_{\|} \rangle$ inferred from the conversion efficiency is significantly larger than those launched by the waveguide array. Such an upshift may be a result of modifications of the launched $n_{\|}$ spectrum due to toroidal effects, and the presence of the negative spectrum ($n_{\|} < 0$).[18]

The evolution of the conversion efficiency with time during a shot can be studied by plotting the experimentally determined conversion efficiency P_{el}/P_{rf} against v_{ph}/v_r with time as the varying parameter, as reported earlier.[7] High efficiency can be obtained for a short time after the rf turn on, but the evaluation of P_{el}/P_{rf} is uncertain during this transient phase, and in any case the high efficiency cannot be sustained for a long time. The value of P_{el}/P_{rf} after the first 50ms is typically 5-10% and generally decreases slowly toward zero along the theoretical curve shown in Fig. 7, as the current approaches the steady state current drive level. It is pos-

sible that in order to optimize the ramp-up, the rf power must also be ramped up with the plasma current so as to maintain the maximum ramp-up efficiency.

The time evolutions of the central electron temperature T_{e0} during LH and OH ramp-up shots, obtained by Thomson scattering on a shot-by-shot basis have been given previously in Ref. [7]. The results have been reproduced in Fig. 8. In addition, the gaussian profile width a_{Te} of the electron temperature profile, as measured by a five channel Thomson scattering system, and the calculated ohmic heating power, V^2/R_{Sp}, for the LH ramp-up case are shown. For the LH ramp-up case, the temperature increases and then decreases on a 50ms time scale. This is much slower than the time scale for the change in the ohmic heating power V^2/R_{Sp}, and the cause is presently not well understood. The electron temperature increases roughly proportional to current for both cases after the first 100ms of the ramp-up. Although the central electron temperature is higher for the RF case, the spatial profile is broader for the OH case so that the stored energies for the two cases are roughly equal. This increase of the electron bulk stored energy with current can be interpreted to be due to increasing P_h (the collisional dissipation of the current carrying tail electrons on the bulk) and/or an improvement of the bulk energy confinement time $\tau_E^{bulk} \equiv (W_e^{bulk} + W_i^{bulk})/(P_h + V^2/R_{Sp})$ with I_p.

Some comments can be made regarding extrapolation of the present results to higher densities. It is seen that experimentally the maximum ramp-up efficiency $\dot{W}/P_{rf}$ is obtained at lowest densities. This may be an indication that even though higher efficiencies at higher densities are still consistent with the theory of Fisch and Karney, the realization of such high efficiencies may not be achievable in practice. As already noted by Fisch and Karney,[10] even if high conversion efficiencies P_{el}/P_{rf} could be obtained at higher densities, higher power levels and higher ramp-up rates (larger $\dot{I}_p$) would be required, which would result in larger ohmic (V^2/R_{Sp}) losses.

Moreover, the problem of impurity influx[6] becomes more severe at high rf power levels and long rf pulse lengths, unless effective impurity control is employed. On the other hand, it may be impractical to reduce the density to the mid to low $10^{18}\,\mathrm{m}^{-3}$ range in future reactor-grade tokamaks. The present results have demonstrated the feasibility of ramping up the current at densities $\overline{n}_e \gtrsim 1 \times 10^{19}\,\mathrm{m}^{-3}$.

C. Transient Effects

The interpretation of ramp-up data during the initial phase is complicated by transient effects. During the build up time of the energetic electron tail, which is typically 2–3ms,[13] $\dot{\beta}_p$ is large. In order to maintain the equilibrium relationship Eq. (3), the vertical field has to increase (with an average feedback response time of 1.4ms) and a significant external voltage, is supplied by the EF circuit. In the present experiments, the rise time of the rf pulse (typically 10ms) determines the build up time of the rf current. This positive voltage allows the edge loop voltage to stay positive (a net inflow of the Poynting flux) while $\dot{I}_p > 0$. A higher ramp-up rate can be obtained during this initial phase compared to the ramp-up rate in the absence of this additional positive loop voltage (see Fig. 1). During this time the external input power P_{ext} is large (see Fig. 4), and the V^2/R_{Sp} loss due to the large negative voltage induced in the plasma interior is also large (see Figs. 1 and 8). If the electrons are heated by this V^2/R_{Sp} power, a better absorption efficiency and/or a better current drive efficiency may be obtained, in principle. However, in the experiment significant electron heating on this time scale was not observed (see Fig. 8). After the electron tail has formed, the external voltage from the EF circuit comes mainly from the $\dot{I}_p$ term, and V_{ext} is reduced to about 2/3 of $\left|-L_{ext}\dot{I}_p\right|$ and the edge loop voltage becomes negative. Thereafter, an almost constant ramp-up rate can be sustained for a longer duration.

III. OH ASSISTED CURRENT RAMP-UP

We have also investigated LH current ramp-up in the presence of OH input power. In a pure OH ramp-up case the power balance can be expressed as $P_{ext} = \dot{W} + V^2/R_{Sp}$ or $V_l I_p = \dot{W}_{int} + V^2/R_{Sp}$, and the electric field is in the forward direction (the direction of I_p). For LH ramp-up in the presence of inductive drive from the OH primary circuit, the electric field need not be negative and we might expect synergistic effects of rf ramp-up and the forward electric field.[6] Such an OH assisted LH ramp-up shot is shown in Fig. 9. The edge loop voltage during the ramp-up was +1 V, but the central loop voltage was estimated to be approximately −0.5 V. A very large ramp-up rate is indeed observed. The ramp-up rate decreases from an initial value of 2MA/s at $t = 250$ ms to 1MA/s at $t = 300$ ms. (In the absence of OH assist, $P_{rf} = 500$ kW is the power required to maintain about 200kA of steady state current at this density.) The decay of plasma current starting at $t \simeq 310$ ms is caused by the inversion of the OH power supply ($P_{ext} < 0$). For the present case, $\dot{W} \simeq P_{rf} \simeq 500$ kW, so that $\dot{W}/P_{rf} \simeq 100\%$. The external input power, P_{ext}, increased only slightly during the ramp-up phase compared to the ohmically maintained phase ($t = 200$–240 ms) and was comparable to P_{rf}. The rf energy can be converted into the poloidal field energy efficiently in this case since the rf energy need not be expended to maintain the plasma. This mode of operation should enable significant reduction of the requirements on the OH transformer.

IV. OH RECHARGING EXPERIMENTS

While ramp-up of the plasma current was obtained by overdriving the rf current with $\dot{I}_{OH} = 0$, it is also possible to recharge the OH transformer coil while maintaining the plasma current constant with LHCD.[8] This can be achieved by either feedback controlling or preprogramming the OH primary current. The power

flow diagram applicable for OH recharging is similar to that shown in Fig. 2, but with P_{ext} flowing out of the plasma and with $\dot{W} = 0$. Unlike the ramp-up case, $\dot{I}_p = 0$, $\dot{I}_{EF} = 0$, and $P_{ext} = -M_{l,OH}\dot{I}_{OH}I_p = V_l I_p < 0$. Since the plasma is maintained in steady state, the recharging efficiency defined as $-V_l I_p/P_{rf} = M_{l,OH}\dot{I}_{OH}I_p/P_{rf}$ can be constant in time. An example of an OH recharging shot is shown in Fig. 10. The OH primary current was preprogrammed for this case. A recharging rate of $\dot{I}_{OH} = 8\,\mathrm{kA/s}$ is obtained for about 150ms with a constant loop voltage of $-0.22V$. Since the initial charge current on the OH coil is typically 10–20kA, full recharging can be accomplished in 1.2–2.5 seconds at this recharging rate. In the present case the plasma current decayed near the end of the rf pulse due to influx of impurities and density increase. The OH recharging can be sustained for a longer time at a reduced recharging rate (i.e., at lower rf powers). The recharging efficiency of about 7% was obtained. The conversion efficiency $P_{el}/P_{rf} = (-V_l I_p + V^2/R_{Sp})/P_{rf}$ for this case is comparable to that obtained during ramp-up under similar conditions.

V. SUMMARY AND CONCLUSIONS

Plasma current ramp-up by lower-hybrid waves has been studied in a high density reactor-relevant regime ($\overline{n}_e \gtrsim 1 \times 10^{19}\,\mathrm{m}^{-3}$) and the feasibility of ramping up the current in the low $10^{19}\,\mathrm{m}^{-3}$ densities, an order of magnitude higher than previously reported,[5] has been demonstrated. In the absence of ohmic input power ($\dot{I}_{OH} = 0$), the ramp-up efficiency is maximized with typically two to three times the rf power required to maintain a steady state current. The maximum ramp-up efficiency $\dot{W}/P_{rf}$ of over 20% is obtained at a density of $\overline{n}_e \simeq 1 \times 10^{19}\,\mathrm{m}^{-3}$. The maximum ramp-up efficiency obtainable is lower at higher densities. The effective absorption efficiency of $\eta_{eff} \simeq 0.6$ (with direct electron tail losses subtracted out) and the average $n_\parallel$ of $\langle n_\parallel \rangle \simeq 3$ adequately describe the experimental conversion

efficiencies when fitted to the theory of Fisch and Karney. This value of $\langle n_{\|} \rangle$, which represents a weighted average of $n_{\|}$ when the waves are absorbed, is significantly higher than typical values of $n_{\|}$ launched by the grill. These values, however, are not unique, and other combinations (e.g., $\eta_{eff} = 1.0$, $\langle n_{\|} \rangle \simeq 4$) can fit the data equally well. Therefore, a more accurate modeling, including the distribution of power spectrum, may eventually be needed for a proper characterization of rampup experiments. The kinetic stored energy was also found to increase during the ramp-up. In the presence of ohmic input power, significantly larger ramp-up rates (in excess of 1MA/s) could be obtained at higher densities and currents.

In OH recharging experiments a steady state plasma can be maintained by rf while the OH transformer is being recharged. The ohmic input power is negative in this case. A recharging rate of 8kA/s was obtained for an input rf power of 510kW, which corresponds to a recharging efficiency of $M_{l,OH}\dot{I}_{OH}I_p/P_{rf} \simeq 7\%$. The conversion efficiency during recharging is comparable with that during ramp-up under similar plasma conditions. Highest recharging efficiencies have been observed at lowest densities. However, adequate recharging rates have been observed at a density of $\overline{n}_e \gtrsim 1 \times 10^{19}\,\mathrm{m}^{-3}$, which may be used in reactor-type devices.

ACKNOWLEDGMENTS

We thank D. Gwinn for assistance with the OH transformer recharging experiments, D. Griffin for maintaining the rf equipment, S. McCool for performing the Thomson scattering experiments, and other members of the Alcator group for their contributions. This work was supported by the U.S. Department of Energy, under Contract No. DE–AC02–78ET51013.

[1]S. Bernabei, C. Daughney, P. Efthimion, W. Hooke, J. Hosea, F. Jobes, A. Martin, E. Mazzucato, E. Meservey, R. Motley, J. Stevens, S. von Goeler, R. Wilson, Phys. Rev. Lett. **49**, 1255 (1982).

[2]M. Porkolab, J. J. Schuss, B. Lloyd, Y. Takase, S. Texter, P. Bonoli, C. Fiore, R. Gandy, D. Gwinn, B. Lipschultz, E. Marmar, D. Pappas, R. Parker, P. Pribyl, Phys. Rev. Lett. 53, 450 (1984).

[3]C. Gormezano, P. Blanc, H. Hottollier, P. Briand, G. Briffod, P. Chabert, M. Clément, A. Girard, W. Hess, G. T. Hoang, G. Ichtchenko, G. Melin, F. Parlage, J. C. Vallet, and D. Van Houtte, in Radio Frequency Plasma Heating (Proc. 6th Top. Conf., Callaway Gardens, GA, 1985) AIP, New York (1985) p. 111.

[4]N. J. Fisch, Phys. Rev. Lett. **41**, 873 (1978); C. F. F. Karney and N. J. Fisch, Phys. Fluids **22**, 1817 (1979); C. F. F. Karney and N. J. Fisch, Phys. Fluids **28**, 116 (1985).

[5]F. C. Jobes, S. Bernabei, T. K. Chu, W. M. Hooke, E. B. Meservey, R. W. Motley, J. E. Stevens, and S. von Goeler, Phys. Rev. Lett. **55**, 1295 (1985).

[6]M. Porkolab, B. Lloyd, J. J. Schuss, Y. Takase, S. Texter, R. Watterson, P. Bonoli, R. Englade, C. Fiore, R. Gandy, R. Granetz, M. Greenwald, D. Gwinn, B. Lipschultz, E. Marmar, S. McCool, D. Pappas, R. Parker, P. Pribyl, J. Rice, J. Terry, and S. Wolfe, in Heating in Toroidal Plasmas (Proc. 4th Int. Symp., Rome, Italy, 1984) Int. School of Plasma Phys., Varenna (1984) Vol. I, p. 529.

[7]Y. Takase, S. Knowlton, S. McDermott, M. Porkolab, S. Texter, C. Fiore, S. McCool, P. Pribyl, J. Rice, in Radio Frequency Plasma Heating (Proc. 6th Top. Conf., Callaway Gardens, GA, 1985) AIP, New York (1985) p. 186.

[8]F. Leuterer, D. Eckhartt, F. Söldner, G. Becker, K. Bernhardi, M. Brambilla, H.

Brinkschulte, H. Derfler, U. Ditte, A. Eberhagen, G. Fussmann, O. Gehre, J. Gernhardt, G. v. Gierke, E. Glock, O. Gruber, G. Haas, M. Hesse, G. Janeschitz, F. Karger, M. Keilhacker, S. Kissel, O. Klüber, M. Kornherr, G. Lisitano, R. Magne, H. M. Mayer, K. McCormick, D. Meisel, V. Mertens, E. R. Müller, M. Münich, H. Murmann, W. Poschenrieder, H. Rapp, F. Ryter, K. H. Schmitter, F. Schneider, G. Siller, P. Smeulders, K. H. Steuer, T. Vien, F. Wagner, F. v. Woyna, and M. Zouhar, Phys. Rev. Lett. **55**, 75 (1985).

[9]N. J. Fisch, in Heating in Toroidal Plasmas (Proc. 3rd Joint Varenna-Grenoble Int. Symp., Grenoble, 1982) CEC, Brussels (1982) Vol. III, p. 841.

[10]N. J. Fisch, C. F. F. Karney, Phys. Rev. Lett **54**, 897 (1985); C. F. F. Karney, N. J. Fisch, Phys. Fluids **29**, 180 (1986).

[11]C. S. Liu, V. S. Chan, and Y. C. Lee, Phys. Rev. Lett. **55**, 2583 (1985).

[12]M. Porkolab, J. J. Schuss, B. Lloyd, Y. Takase, S. Texter, R. Watterson, P. Bonoli, R. Englade, C. Fiore, R. Gandy, R. Granetz, M. Greenwald, D. Gwinn, B. Lipschultz, E. Marmar, S. McCool, D. Pappas, R. Parker, P. Pribyl, J. Rice, J. Terry, S. Wolfe, R. Slusher, and C. M. Surko, in Radio Frequency Plasma Heating (Proc. 5th Top. Conf., Madison, Wisconsin, 1983) Univ. Wisconsin, Madison (1983) p. 88.

[13]S. Texter, Ph. D. Thesis, Massachusetts Institute of Technology (1986).

[14]S. Knowlton, M. Porkolab, Y. Takase, S. Texter, P. Bonoli, C. Fiore, S. McCool, F. S. McDermott, and J. L. Terry, Phys. Rev. Lett. **57**, 587 (1986); Y. Takase, P. Bonoli, S. Knowlton, M.Porkolab, S. Texter, C. Fiore, S. McCool, S. McDermott, and J. Terry, accepted for publication in Nucl. Fusion.

[15]C. F. F. Karney, N. J. Fisch, F. C. Jobes, Phys. Rev. A **32**, 2554 (1985).

[16]V. D. Shafranov, in Review of Plasma Physics, Vol. 2, ed. by M. A. Lentovich,

Consultants Bureau, New York (1966) p. 103.

[17]S. Texter, S. Knowlton, M. Porkolab, and Y. Takase, accepted for publication in Nucl. Fusion.

[18]P. Bonoli, R. Englade, and M. Porkolab, in Heating in Toroidal Plasmas (Proc. 4th Int. Symp., Rome, Italy, 1984) Int. School of Plasma Phys., Varenna (1984) Vol. II, p. 1311.

FIGURE CAPTIONS

FIG. 1. A typical LH current ramp-up shot. Hydrogen plasma, $B = 8.2\,\mathrm{T}$, $\overline{n}_e = 2.3 \times 10^{19}\,\mathrm{m}^{-3}$, $P_{rf} = 420\,\mathrm{kW}$. The solid loop voltage trace is the measured loop voltage at the edge, while the dashed trace is the calculated loop voltage at the plasma center.

FIG. 2. A schematic diagram of the power flow during LH current ramp-up. Note that $P_{in} = P_{abs} - P_{loss} = P_{el} + P_h$.

FIG. 3. An equivalent circuit diagram during LH current drive. Note that $I_p = I_{rf} + V/R_{Sp}$ where $V < 0$ during ramp-up and OH recharging.

FIG. 4. The rf power (dash-dot line), $\dot{W}$ (solid line), and P_{ext} (dotted line) as functions of time. Hydrogen, $B = 8.2\,\mathrm{T}$, $\overline{n}_e = 1.6 \times 10^{19}\,\mathrm{m}^{-3}$, $P_{rf} = 260\,\mathrm{kW}$.

FIG. 5. The time averaged current ramping efficiency $\dot{W}/P_{rf}$ as a function of rf power. Hydrogen plasma, $B = 8.2\,\mathrm{T}$, $\overline{n}_e = (2.0\text{–}2.5) \times 10^{19}\,\mathrm{m}^{-3}$, initial $I_p = 90\,\mathrm{kA}$.

FIG. 6. The maximum time averaged current ramping efficiency $\dot{W}/P_{rf}$ as a function of density. Hydrogen plasma, $B = 8.2\,\mathrm{T}$.

FIG. 7. Comparison of the time averaged conversion efficiency P_{el}/P_{rf} with the Fisch-Karney theory. Hydrogen plasma, $B = 8.2\,\mathrm{T}$. The theoretical curves are for $Z_{eff} = 3$, (a) $\eta_{eff} = 0.6$, $\langle n_\parallel \rangle \simeq 3$, and (b) $\eta_{eff} = 1.0$, $\langle n_\parallel \rangle \simeq 4$.

FIG. 8. Time evolution of the central electron temperature T_{e0} and the electron temperature profile width a_{Te} during LH and OH current ramp-up plasmas.

Hydrogen plasma, $B = 8.2\,\mathrm{T}$, $\overline{n}_e = (2.5\text{–}3.0) \times 10^{19}\,\mathrm{m}^{-3}$, $P_{rf} = 450\text{–}530\,\mathrm{kW}$. Also shown is the ohmic power loss V^2/R_{Sp} for the LH ramp-up plasma.

FIG. 9. OH assisted LH ramp-up shot. Hydrogen plasma, $B = 8.2\,\mathrm{T}$, $\overline{n}_e = 3.2 \times 10^{19}\,\mathrm{m}^{-3}$, $P_{rf} = 500\,\mathrm{kW}$.

FIG. 10. OH recharging shot. Hydrogen plasma, $B = 9.8\,\mathrm{T}$, $I_p = 150\,\mathrm{kA}$, $\overline{n}_e = 1.6 \times 10^{19}\,\mathrm{m}^{-3}$, $P_{rf} = 510\,\mathrm{kW}$.

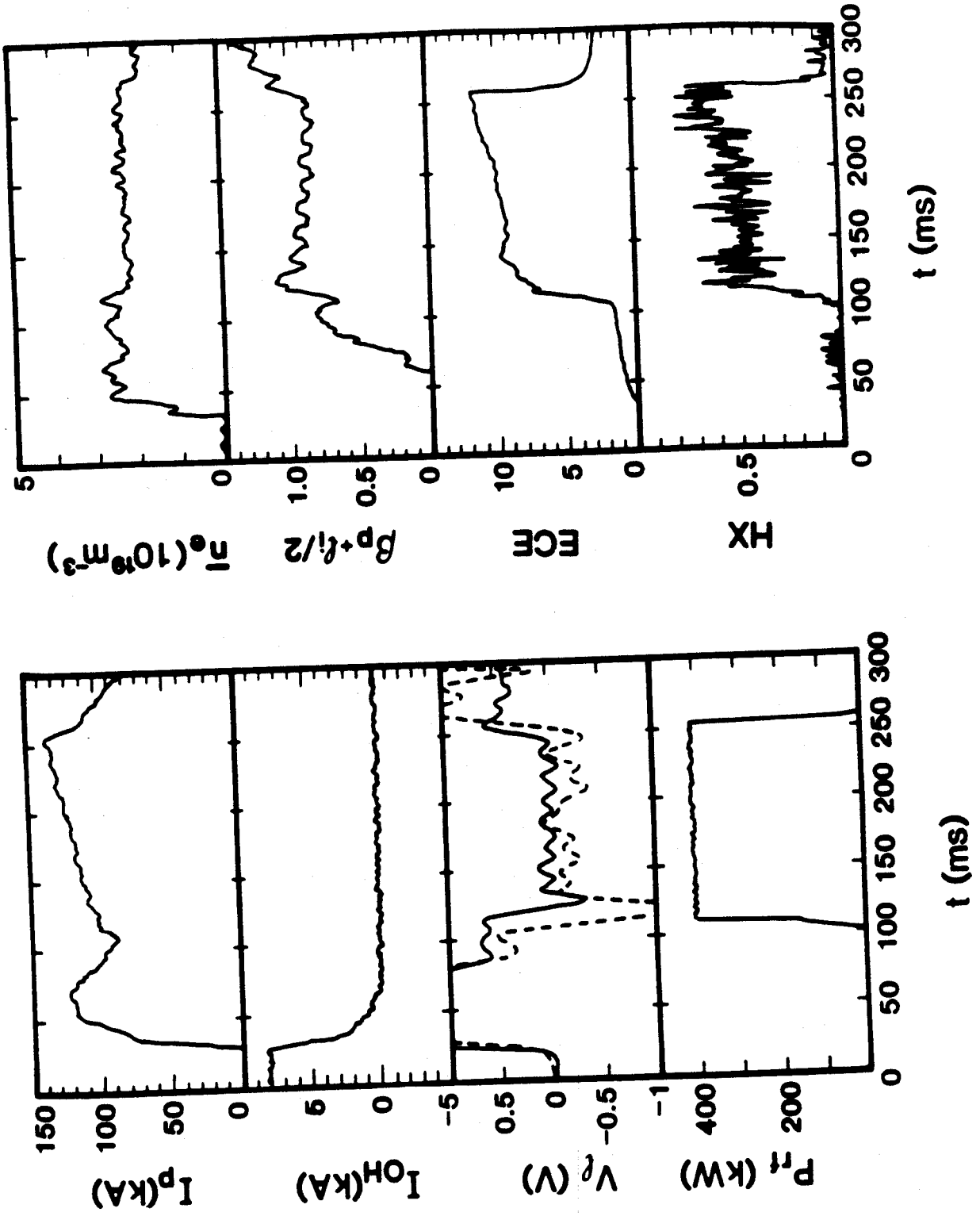
HX
ECE
$\beta_{p+\ell i}/2$
$\bar{n}_e(10^{19}m^{-3})$
P_{rf} (kW)
V_ℓ (V)
I_{OH}(kA)
I_p(kA)
t (ms)
t (ms)

Fig. 1

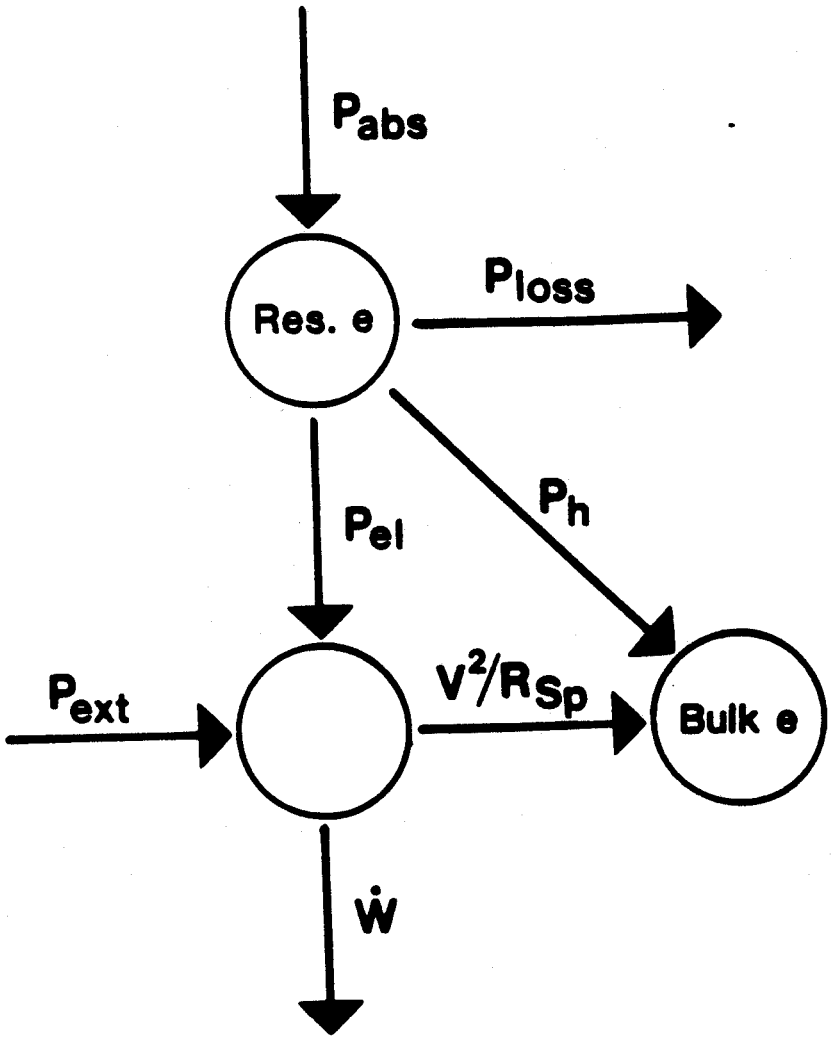

Fig. 2

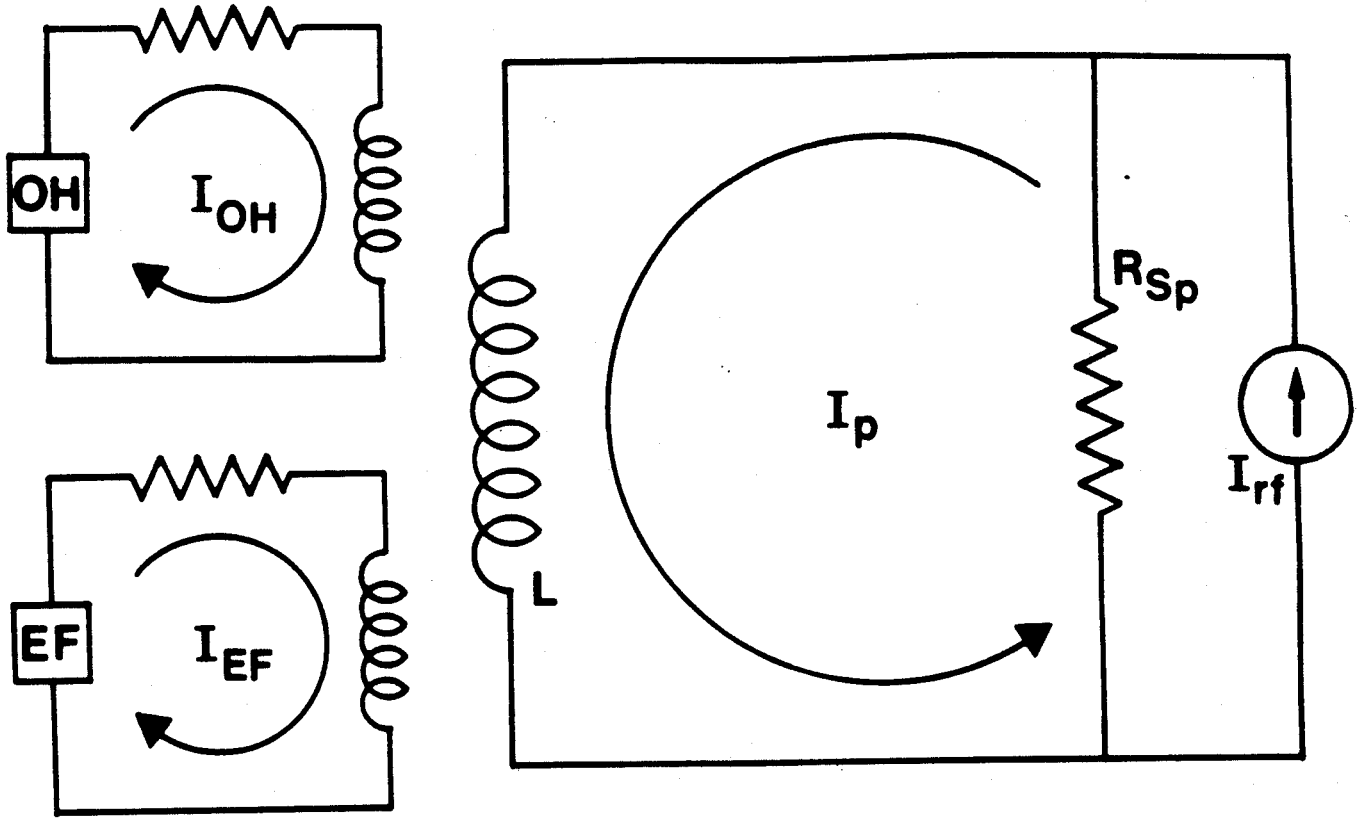

Fig. 3

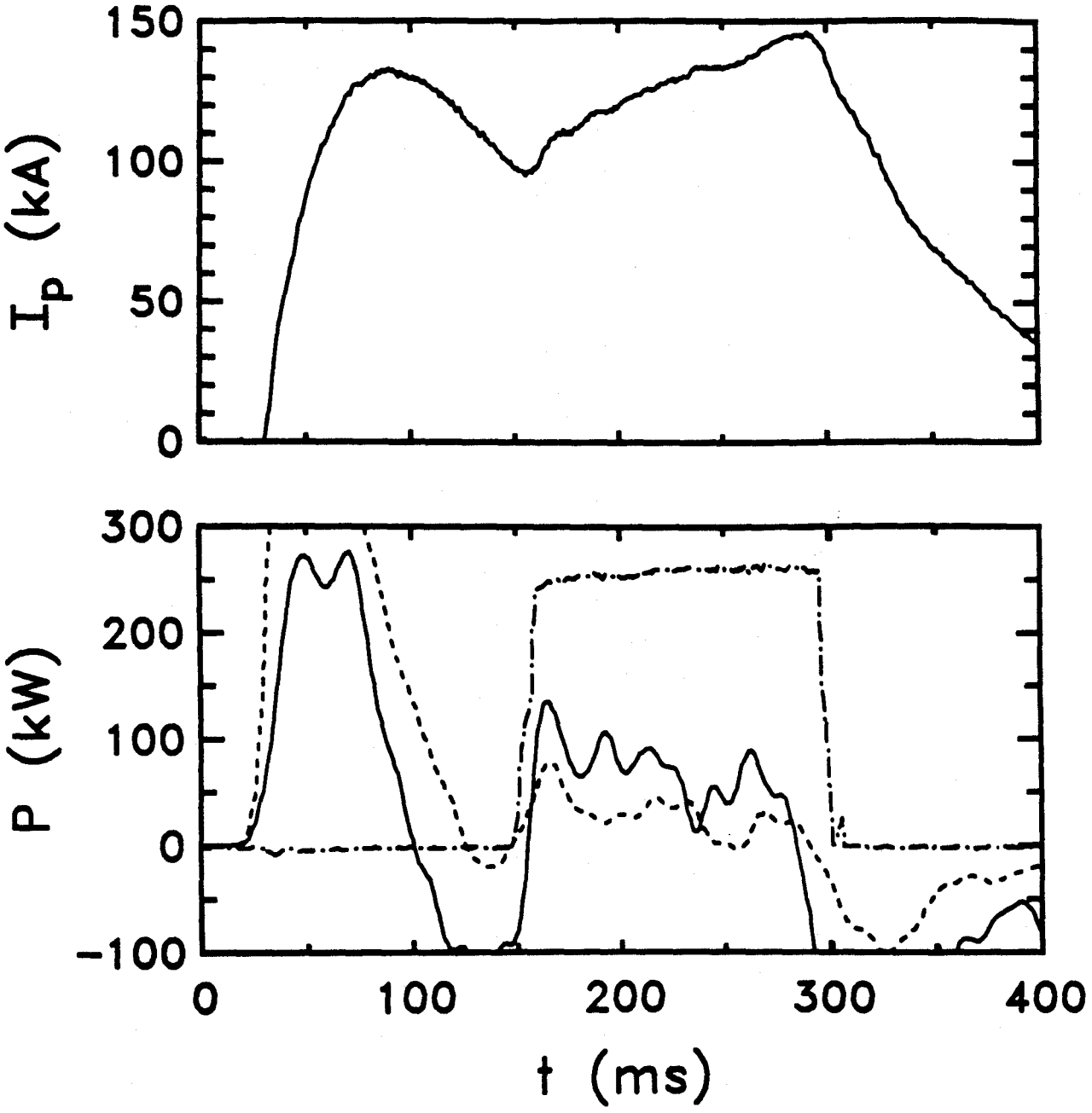

Fig. 4

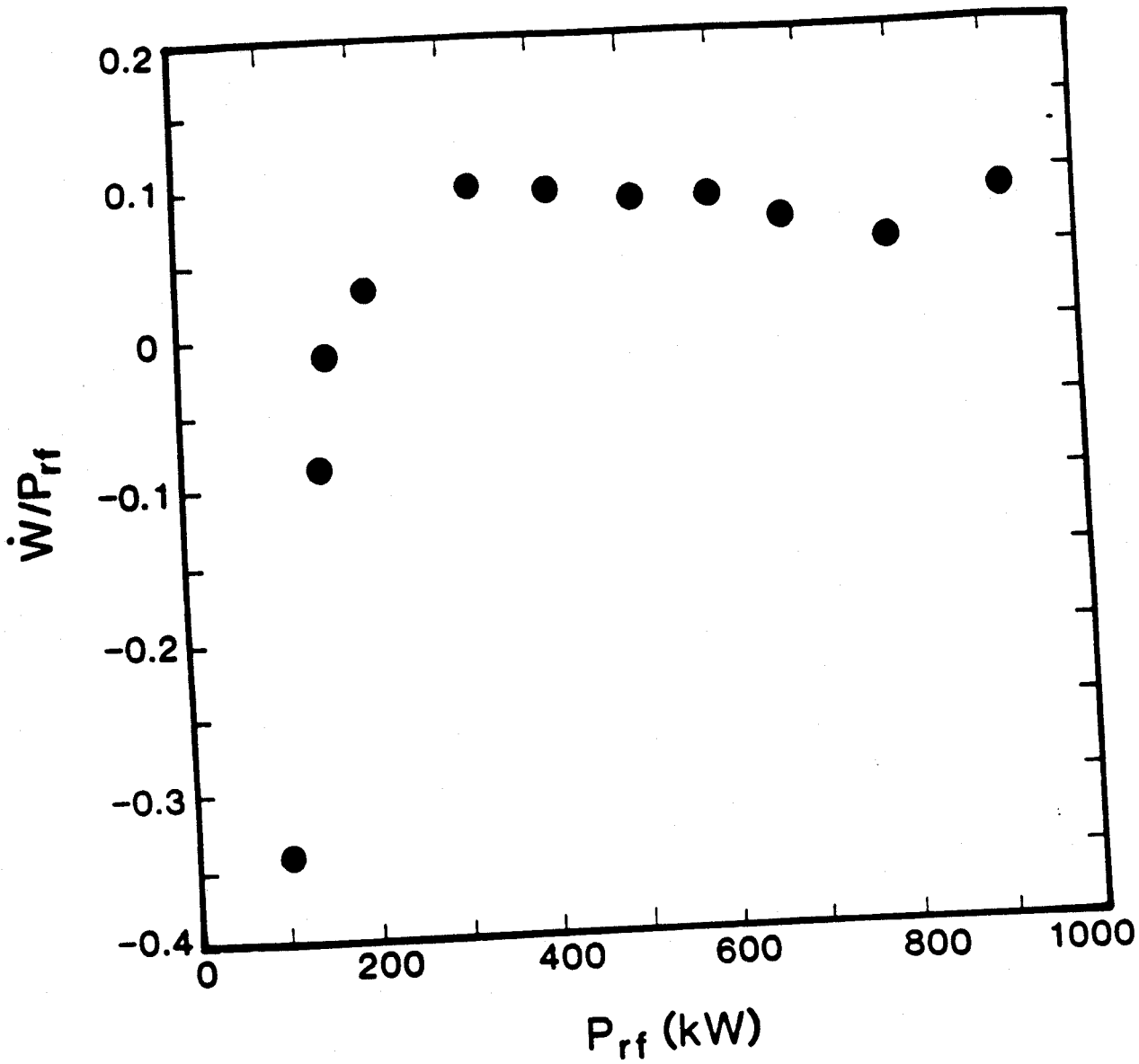

Fig. 5

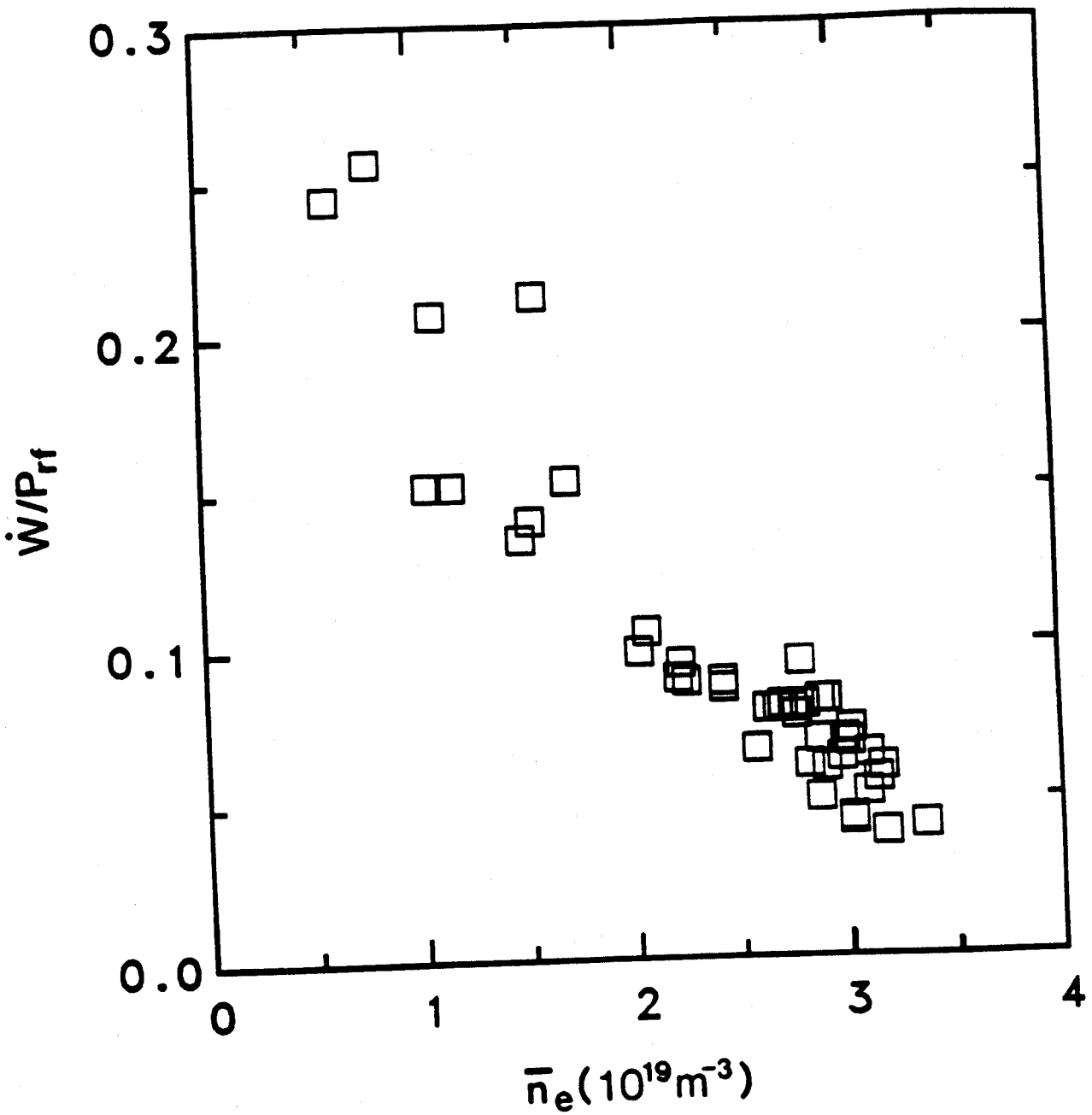

Fig. 6

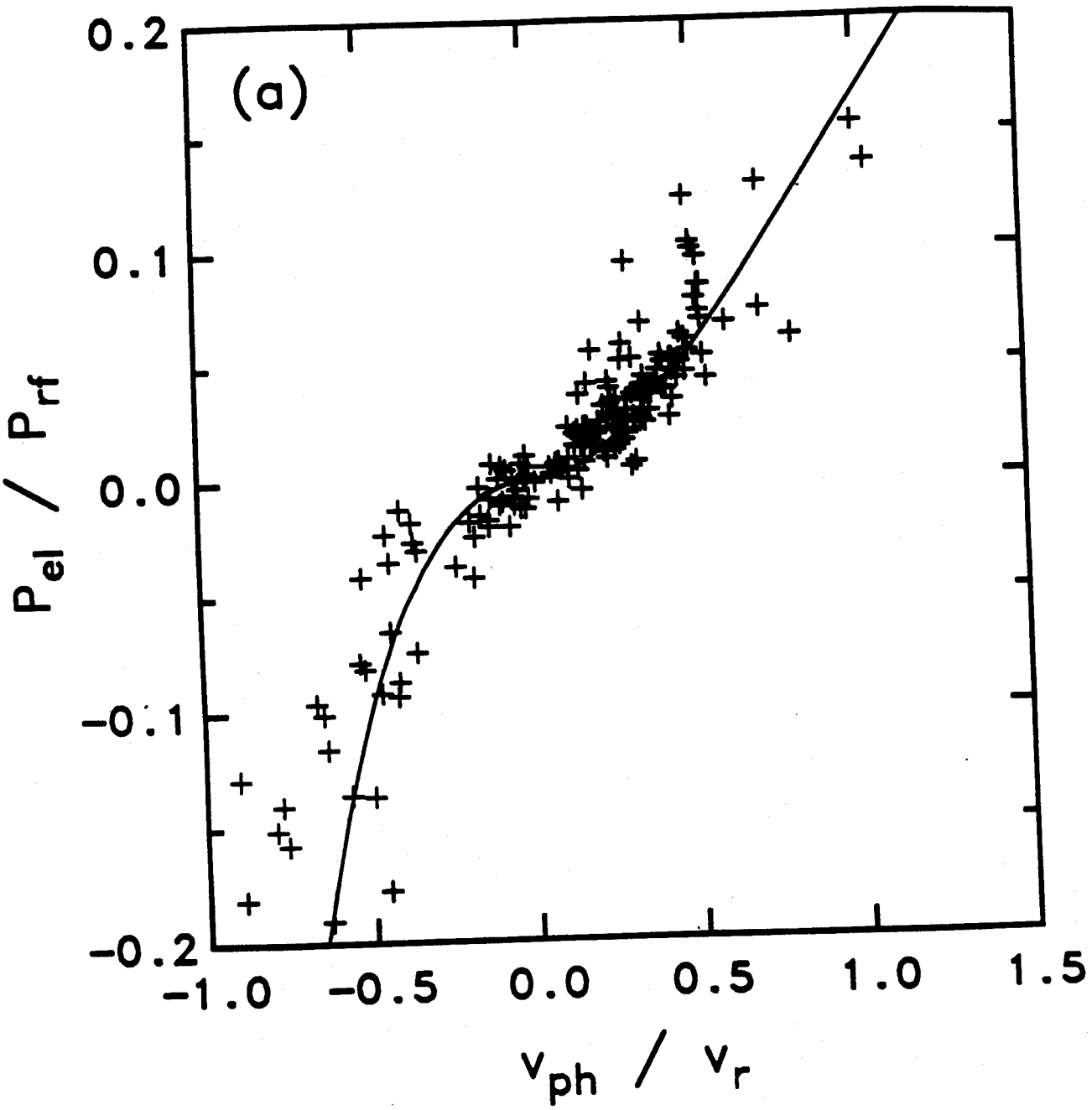

Fig. 7(a)

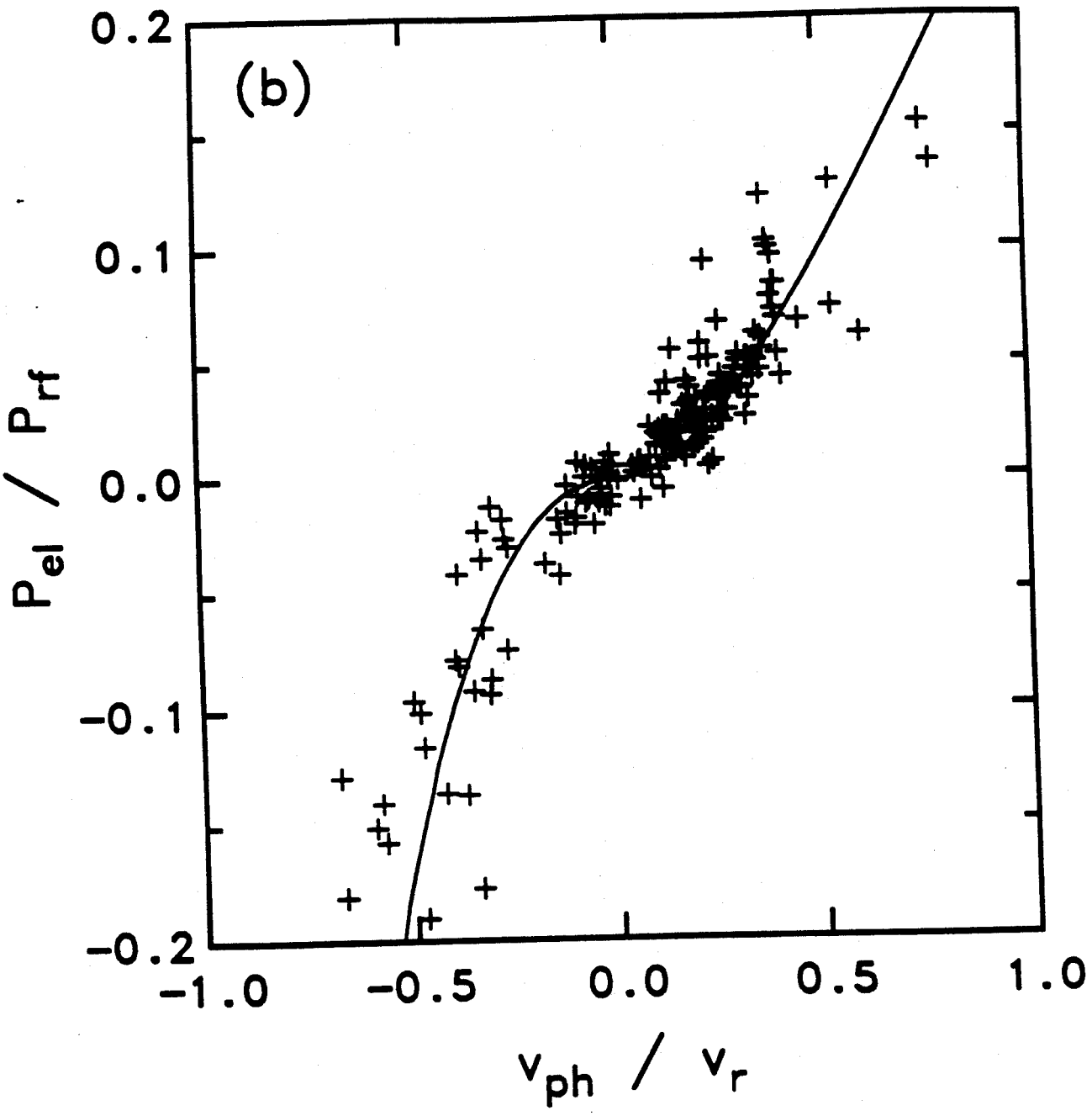

Fig. 7(b)

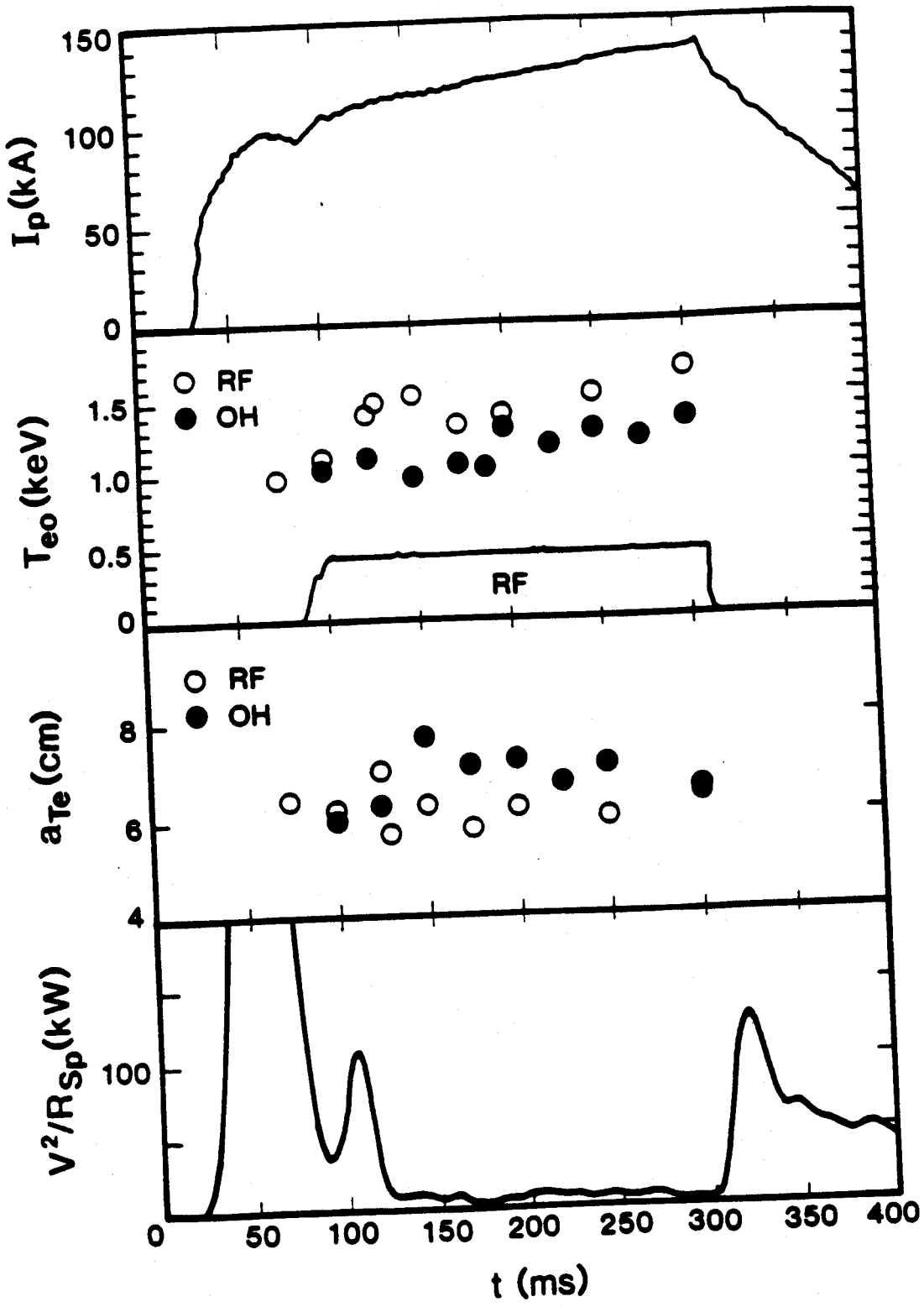
150
100
50
0
I_p(kA)
RF
OH
1.5
1.0
0.5
0
T_{eo}(keV)
RF
RF
OH
8
6
a_{Te}(cm)
4
100
V^2/R_{Sp}(kW)
0
50
100
150
200
250
300
350
400
t (ms)

Fig. 8

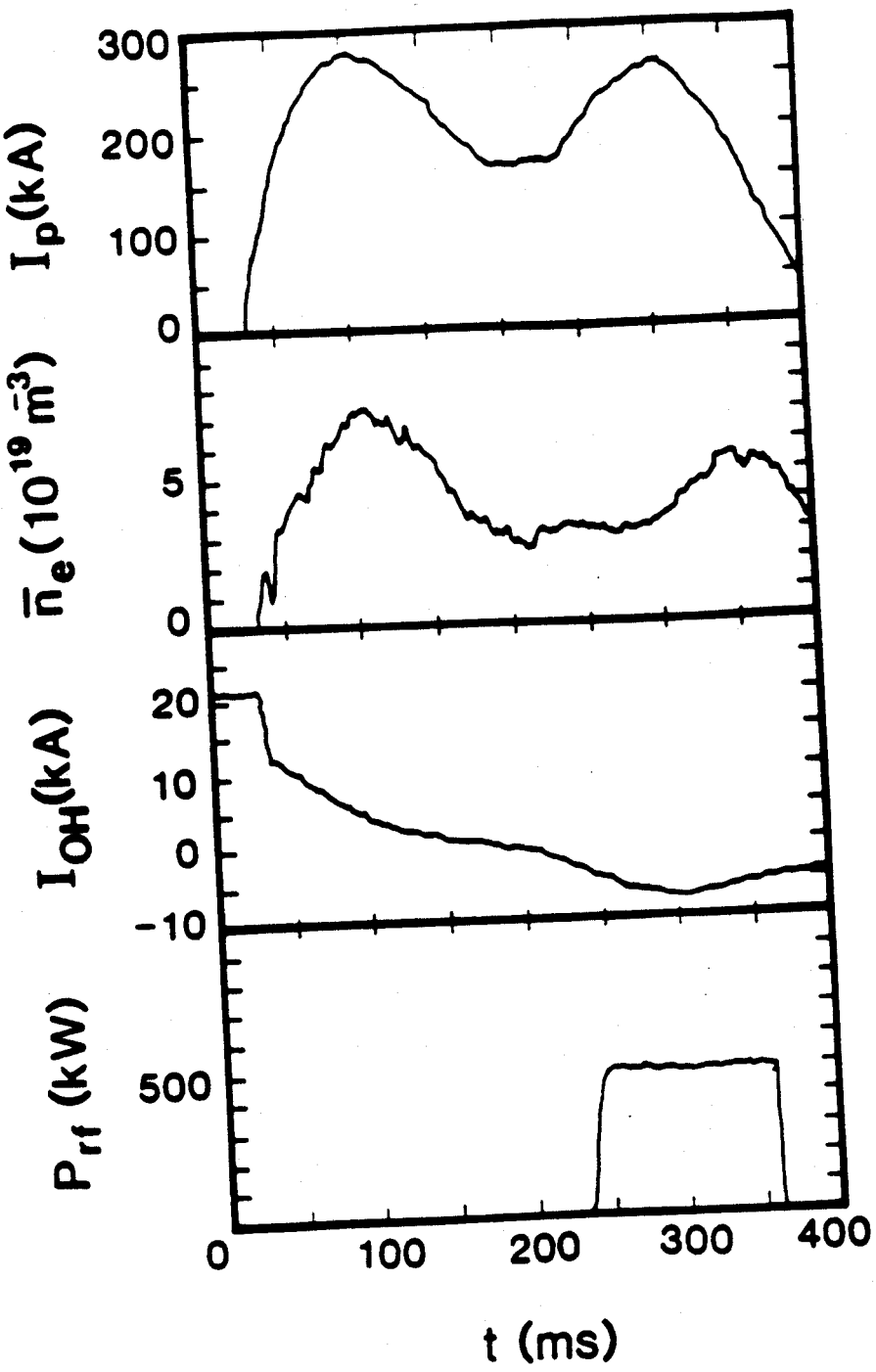
300
200
100
0
I_p(kA)
5
0
$\bar{n}_e(10^{19}\,m^{-3})$
20
10
0
-10
I_{OH}(kA)
500
P_{rf} (kW)
0
100
200
300
400
t (ms)

Fig. 9

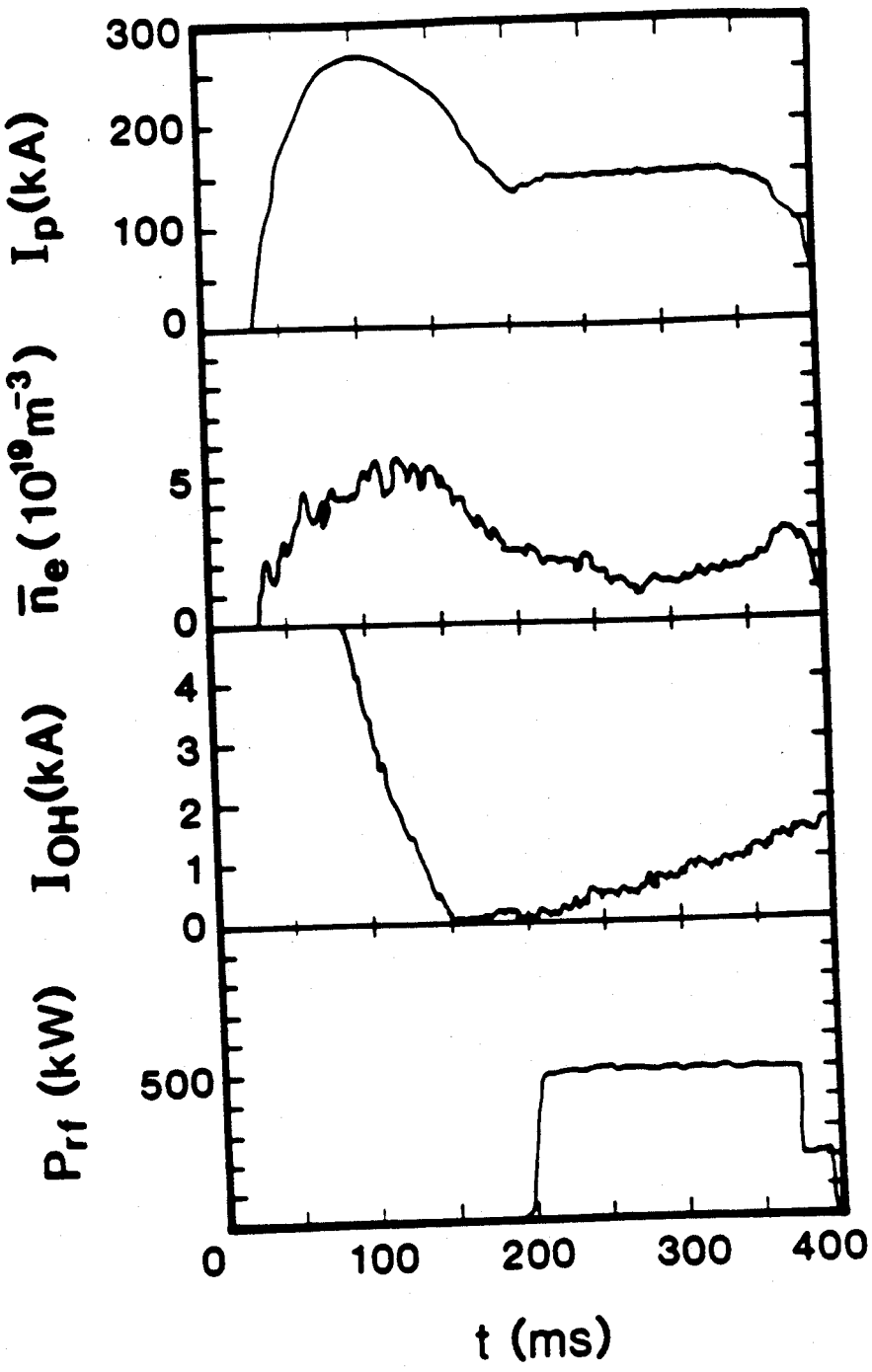
300
200
100
0
I_p(kA)
5
0
$\bar{n}_e$(10^{19}m^{-3})
4
3
2
1
0
I_{OH}(kA)
500
P_{rf} (kW)
0
100
200
300
400
t (ms)

Fig. 10